Stellar dynamos and cycles from numerical simulations of convection*

Caroline Dubé† & Paul Charbonneau

Université de Montréal, † dube@astro.umontreal.ca

We present a series of kinematic axisymmetric mean-field $\alpha\Omega$ dynamo models applicable to solar-type stars, for 20 distinct combinations of rotation rates and luminosities. The internal differential rotation and kinetic helicity profiles required to calculate source terms in these dynamo models are extracted from a corresponding series of global three-dimensional hydrodynamical simulations of solar/stellar convection, so that the resulting dynamo models end up involving only one free-parameter, namely the turbulent magnetic diffusivity in the convecting layers. Even though the $\alpha\Omega$ dynamo solutions exhibit a broad range of morphologies, and sometimes even double cycles, these models manage to reproduce relatively well the observationally-inferred relationship between cycle period and rotation rate. On the other hand, they fail to capture the observed increase of magnetic activity levels with rotation rate. This failure is due to our use of a simple algebraic α-quenching formula as the sole amplitude-limiting nonlinearity. This suggests that α-quenching is not the primary mechanism setting the amplitude of stellar magnetic cycles, with magnetic-reaction on large-scale flows emerging as the more likely candidate. This inference is coherent with analyses of various recent global magnetohydrodynamical simulations of solar/stellar convection.

Since the mid-1960s, data on cyclic magnetic activity has been obtained from the Mt Wilson survey of chromospheric emission (Ca II H & K bands) in a sample of nearby solar-type stars. Analyses of these data has led to the determination of various empirical relationships linking fundamental stellar parameters to cycle periods ($P_{\rm cyc}$), mean chromospheric H-K flux ratio ($\langle R'_{\rm HK}\rangle$), and more recently X-ray-to-bolometric luminosity ratio (R_X). Not surprisingly, attempts to model stellar cycles using dynamo models can lead to a wide variety of results, depending on the assumptions made. **We use hydrodynamical simulations of convection (using EULAG model) to produce large-scale flow and α-tensor profiles that are then used as input to kinematic mean-field $\alpha\Omega$ dynamo models.**

Rotation affects convective velocities. The convective energy flux increases with increasing Ro more slowly than one would expect from its rotational dependence.

Smaller t_s drives more vigorous convection

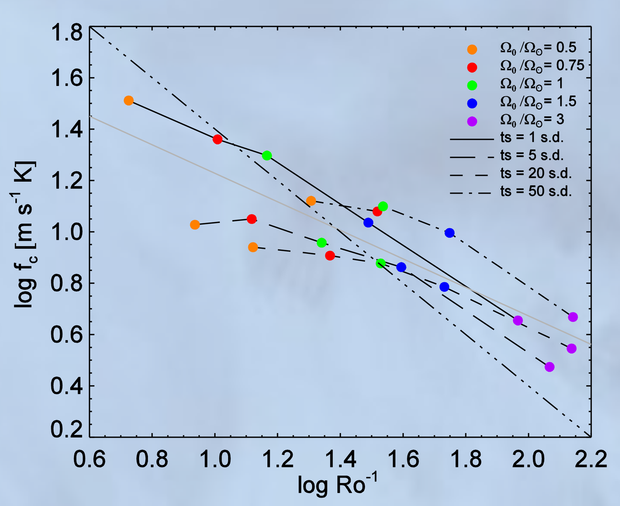

$$\mathrm{Ro} = \frac{u'_{r\,\rm rms}}{\Omega_0 L}$$

- Variation of the convective thermal flux f_c at $r/R = 0.85$ vs. inverse Rossby number Ro^{-1}
- Color of symbols: rotation rate; Line segment style: thermal forcing timescale
- Well-fit by a power-law with index -0.56 (grey line)
- Differs from -1 (dashed-triple-dot straight line): convective energy transport affected by rotation

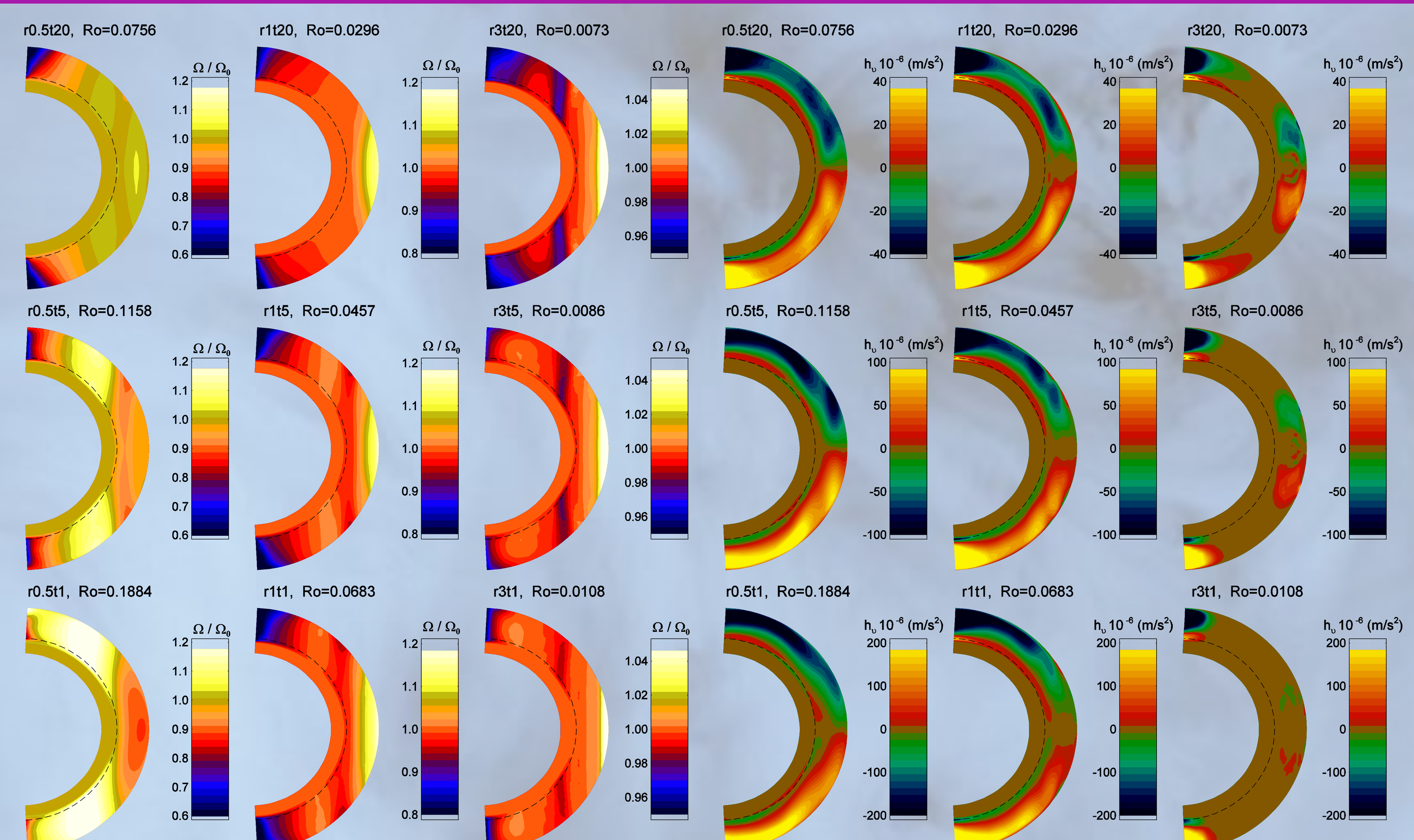

- Differential rotation profiles (left) and mean kinetic helicity profiles (right).
- Rotation rate, left to right: $\Omega_0/\Omega_\odot = 0.5, 1$ and 3
- Timescale for thermal forcing, bottom to top: $t_s = 1, 5$ and 20
- Dashed line, base of the convective zone
- Differential rotation profiles: - normalized according to the rotation rate Ω_0
  - color scale, black (slower than Ω_0) to white (faster than Ω_0)
  - solar-like surface differential rotation profile
  - isocontours, too strong alignment with the rotation axis
  - alignment most pronounced, small t_s or high Ω_0
  - no clear relationship to Ro
- Mean kinetic helicity profiles: - color scale indicates the magnitude and sign of h_v in m s^{-2}
  - range increasing from top to bottom
  - peak in polar regions and secondary extrema at low latitudes
  - negative (positive) in the Northern (Southern) hemisphere
  - sign change near the base of the convection zone

Validation of our $\alpha\Omega$ mean-field dynamo model. **We can capture the main features of a global MHD simulation run at the same rotation rate and forcing timescale.**

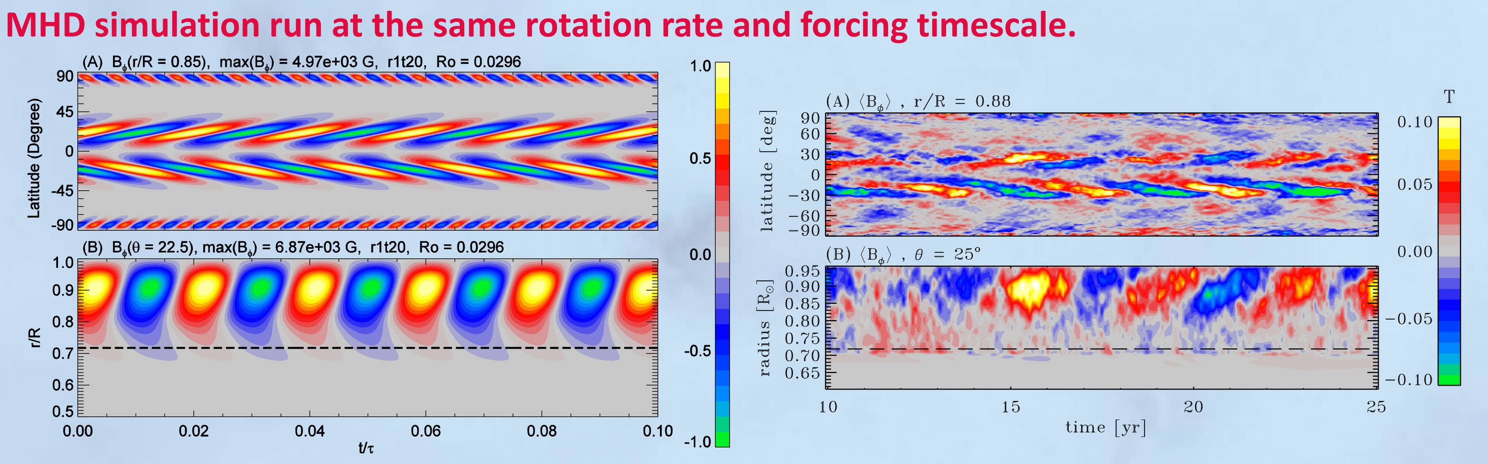

- Spatiotemporal evolution of the zonally-averaged toroidal magnetic field for the $\alpha\Omega$ model constructed from solution `r1t20` (left) and for a EULAG-MHD simulation otherwise identical
- Top panels, time-latitude diagram at $r/R = 0.85$ (left) and $r/R = 0.88$ (right)
- Bottom panels, time-radius diagram at 22.5° latitude (left) and 25° latitude (right)
- Dashed line, base of the convective zone
- $\alpha\Omega$ dynamo solution: - color scale codes the normalized magnetic field strength
  - primary dynamo mode: - concentrated at low latitudes
    - antisymmetric with respect to the equator
    - migrates poleward
  - second, shorter cycle at polar latitudes
  - both modes peaking at $r/R \approx 0.9$ and migrating upward
- MHD solution: - color scale denotes the magnetic field strength in Tesla
  - cycle located at low latitudes, antisymmetric relative to the equator, peaking at $r/R \approx 0.9$ and migrating upward

Physical parameters extracted or used for each simulation

Name[a]	$\Omega_0/\Omega_\odot$	t_s [s.d.]	$u'_{r\,\rm rms}$ [m s^{-1}][b]	Ro[c]	f_c [m s^{-1} K][d]	η_0 [m^2 s^{-1}][e]	$D_{\rm crit}$[f]	$P_{\rm cyc}$ [d][g]	$P_{\rm cyc}(2)$ [d][g]	$E_{\rm mag}$ [$\times 10^{27}$ J][h]
r0.5t1	0.5	1	40.8	0.1884	32.5	1.6e9	185	-	-	2153
r0.5t5	0.5	5	25.1	0.1158	10.7	1.0e9	3050	41.86	-	260
r0.5t20	0.5	20	16.4	0.0756	8.7	6.3e8	16500	84.54	-	405
r0.5t50	0.5	50	10.7	0.0494	13.2	5.3e8	17500	33.22	-	5
r0.75t1	0.75	1	31.8	0.0981	22.9	1.1e9	3600	58.94	-	813
r0.75t5	0.75	5	24.8	0.0763	11.2	8.6e8	9250	36.55	54.13	294
r0.75t20	0.75	20	13.9	0.0430	8.1	5.5e8	7350	119.22	-	158
r0.75t50	0.75	50	9.8	0.0303	12.0	5.0e8	13500	126.65	-	179
r1t1	1	1	29.5	0.0683	19.8	9.4e8	5750	57.82	33.00	303
r1t5	1	5	19.8	0.0457	9.1	7.0e8	5500	87.98	-	196
r1t20	1	20	12.8	0.0296	7.5	5.1e8	8750	108.22	29.61	63
r1t50	1	50	12.6	0.0291	12.6	1.0e9	42500	43.47	262.87	2886
r1.5t1	1.5	1	21.1	0.0324	10.9	6.6e8	9500	133.72	-	485
r1.5t5	1.5	5	16.5	0.0255	7.3	5.8e8	8750	108.93	-	133
r1.5t20	1.5	20	12.0	0.0186	6.1	5.1e8	10000	165.82	-	226
r1.5t50	1.5	50	11.6	0.0179	9.9	1.0e9	43000	76.57	76.57	824
r3t1	3	1	14.0	0.0108	4.5	3.9e8	13000	-	-	25
r3t5	3	5	11.1	0.0086	3.0	3.6e8	26500	258.50	-	561
r3t20	3	20	9.5	0.0073	3.5	3.5e8	19000	73.31	-	16
r3t50	3	50	9.4	0.0072	4.7	4.2e8	25500	74.82	-	35

[a] Simulation code name. The first number corresponds to the rotation rate of the stable layer (column 2) and the last number corresponds to the thermal forcing timescale (column 3).
[b] rms (zonal, latitudinal and temporal) average of the radial small-scale flow at mid-convective zone depth
[c] Rossby number defined by $\mathrm{Ro} = u'_{r\,\rm rms}/\Omega_0 L$, where L is the thickness of the convective zone
[d] Convective thermal flux at mid-convection zone
[e] (Turbulent) magnetic diffusivity defined by $\eta_0 = \frac{\tau}{3}(u'_{\rm rms})^2$
[f] Critical dynamo number
[g] Main and secondary cycle period
[h] Magnetic energy

The magnitude of differential rotation varies with thermal forcing timescale and rotation rate.
- Angular velocity contrast:
  $$\Delta\Omega = \max(\Omega(r,\theta)) - \min(\Omega(r,\theta))$$
- Slope shallower than -1, **$\Delta\Omega$ increases with Ω_0**
- Similar to Brown et al. (2008): $\Delta\Omega \propto \Omega_0^{0.3}$

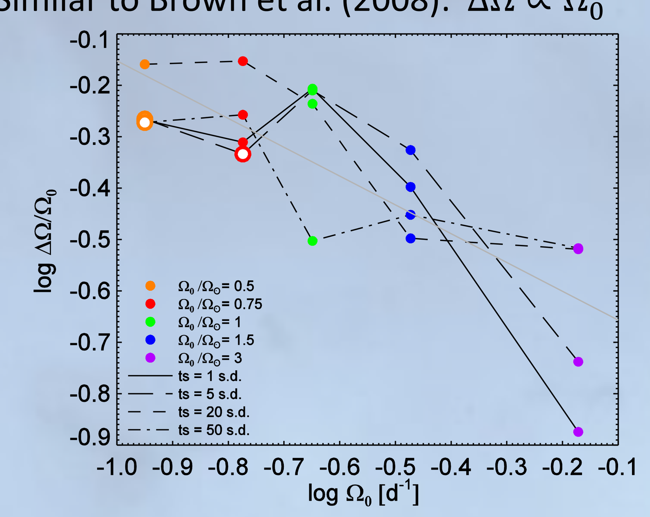

- Differential rotation contrast $\Delta\Omega/\Omega_0$ vs. rotation rate Ω_0
- Open symbols, simulations without equatorial acceleration
- $\Delta\Omega/\Omega_0 \propto \Omega_0^{-0.56}$ (grey line), all points
- $\Delta\Omega/\Omega_0 \propto \Omega_0^{-0.69}$ (fit not shown), omitting simulations without equatorial acceleration

More dynamo solutions across parameter space. Even in the context of our very simple $\alpha\Omega$ formulation a **wide variety of dynamo modes** can be produced.

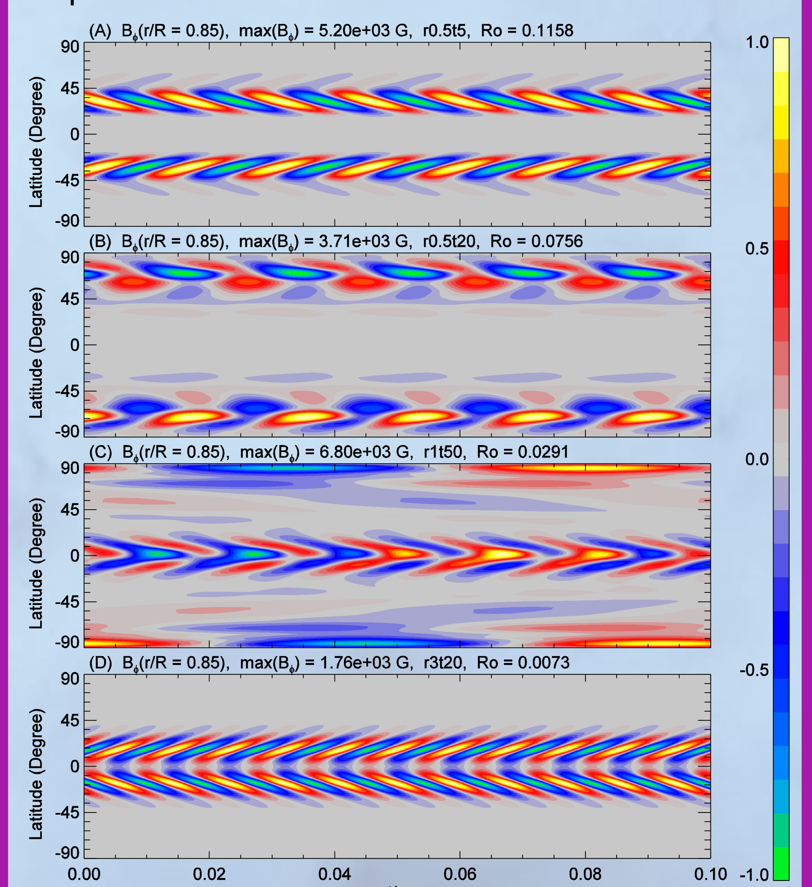

- Kinematic axisymmetric $\alpha\Omega$ dynamo model in spherical geometry
- Mean (large-scale and axisymmetric) magnetic field:
  $$\langle \boldsymbol{B}\rangle(r,\theta,t) = \nabla\times\left(A(r,\theta,t)\hat{\mathbf{e}}_\phi\right) + B(r,\theta,t)\hat{\mathbf{e}}_\phi$$
- B, toroidal component; $\nabla\times\left(A\hat{\mathbf{e}}_\phi\right)$, poloidal component
- Mean (axisymmetric) zonal flow, with $\varpi = r\sin\theta$, no meridional flow:
  $$\langle \boldsymbol{u}\rangle(r,\theta) = \varpi\Omega(r,\theta)\hat{\mathbf{e}}_\phi$$
- Dimensionless evolution equations for A and B in the $\alpha\Omega$ limit:
  $$\frac{\partial A}{\partial t} = \eta\left(\nabla^2 - \frac{1}{\varpi^2}\right)A + C_\alpha \alpha B$$
  $$\frac{\partial B}{\partial t} = \eta\left(\nabla^2 - \frac{1}{\varpi^2}\right)B + \frac{1}{\varpi}\left(\frac{\mathrm{d}\eta}{\mathrm{d}r}\right)\frac{\partial(\varpi B)}{\partial r} + C_\Omega\varpi\left(\nabla\times A\hat{\mathbf{e}}_\phi\right)\cdot(\nabla\Omega)$$
- $C_\alpha = \alpha_0 R/\eta_0$; $C_\Omega = \Omega_0 R^2/\eta_0$
- R, solar radius; α_0, Ω_0, and η_0, characteristic scaling values
- Coefficient α: - $\phi\phi$ component of the full α-tensor
  - Second-Order Correlation Approximation (SOCA; based on a result of Racine et al. 2011):
  $$\alpha = -\frac{\tau}{3}\langle \boldsymbol{u}'\cdot\nabla\times\boldsymbol{u}'\rangle = -\frac{\tau}{3}h_v$$
  - h_v, mean kinetic helicity
  - τ, correlation time of the turbulence: $\tau = H_\rho/u'_{\rm rms}$
  - H_ρ, density scale height of the background stratification
  - $u'_{\rm rms}$, rms average (zonally, latitudinally and temporally) of the small-scale part of the flow velocity
- Amplitude-limiting nonlinearity, algebraic α-quenching:
  $$\alpha \longrightarrow \frac{\alpha}{1+\left(B/B_{\rm eq}\right)^2}$$
- $B_{\rm eq} \propto u'_{\rm rms}$, equipartition field strength

We successfully reproduce the trend linking $P_{\rm cyc}/P_{\rm rot}$ to $1/P_{\rm rot}$.

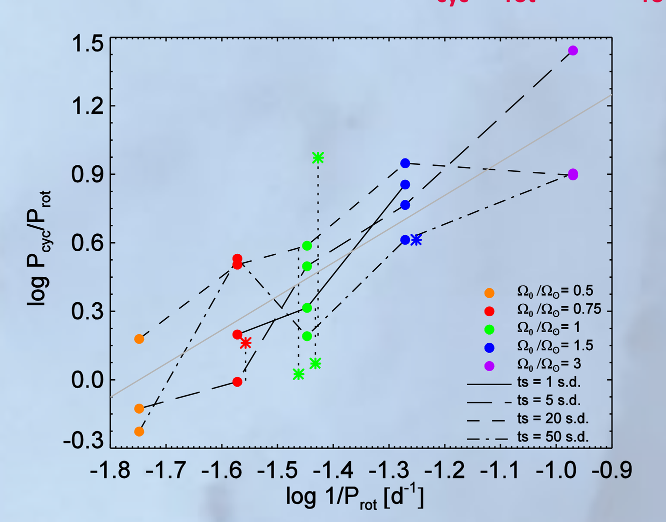

- Variation of the ratio $P_{\rm cyc}/P_{\rm rot}$ with $1/P_{\rm rot}$
- Circles and asterisks, main and secondary cycle respectively
- Vertical dotted lines, link secondary cycles to primary ones
- Asterisks displaced horizontally for clarity
- $P_{cyc}/P_{rot} \propto P_{rot}^{-1.47}$ (grey line) neglects secondary cycles
- Coherent with the results of Baliunas et al. (1996) (slope of -0.74) and Oláh et al. (2009) (slope of -0.81 ± 0.05)

Conclusion

- **Double cycles appear naturally for rotation rates near solar.**
- **The equator-to-pole angular velocity contrast increases moderately with increasing rotation rate.**
- **The general decrease of the cycle period with increasing rotation rate is a very robust property of $\alpha\Omega$ dynamo models, which does not depend sensitively on details of the dynamo mode.**
- **Failure to reproduce the relationship relating the activity level to the Rossby number, suggesting that α-quenching is not the primary amplitude-limiting nonlinearity.**

References

Baliunas, S. L., Nesme-Ribes, E., Sokoloff, D. & Soon, W. H. 1996, ApJ, 460, 848
Brown, B. P., Browning, M. K., Brun, A. S., Miesch, M. S. & Toomre, J. 2008, ApJ, 689, 1354
Oláh, K., Kolláth, Z., Granzer, T. et al. 2009, A&A, 501, 703
Racine, É., Charbonneau, P., Ghizaru, M., Bouchat, A. & Smolarkiewicz, P. K. 2011, ApJ, 735, 46

*Based on a paper by the same title submitted to *The Astrophysical Journal* on May 22nd, 2013. Preprint available on demand.